Received: 3 July 2018 | Revised: 15 August 2018 | Accepted: 21 August 2018

DOI: 10.1002/aoc.4601

WILEY Applied Organometallic Chemistry

FULL PAPER

Design, synthesis and X-ray structural studies of novel [acetonitrile-benzyl-3-N-(2, 4 dihydroxyphenylmethylene) hydrazinecarbodithioato-κ3-N′, S, O] nickel(ll) complex that potently inhibit cell proliferation through regulation of apoptosis related genes

Ronok Zahan[1] | Md. Sifat Rahi[2] | Md. Chanmiya Sheikh[3] | Ryuta Miyatake[3] | Ennio Zangrando[4] | Tarannum Naz[1] | Md. Al-Amin-Al-Azadul Islam[5] | Md Abu Reza[2]

[1]Department of Pharmacy, University of Rajshahi, Rajshahi 6205, Bangladesh

[2]Department of Genetic Engineering and Biotechnology, University of Rajshahi, Rajshahi 6205, Bangladesh

[3]Department of Applied Chemistry, Faculty of Engineering, University of Toyama, 3190 Gofuku, Toyama 930-8555, Japan

[4]Department of Chemical and Pharmaceutical Sciences, Via L. Giorgieri 1, 34127 Trieste, Italy

[5]Department of Chemistry, Rajshahi University of Engineering & Technology, Rajshahi 6204, Bangladesh

Correspondence
Md Abu Reza, PhD, Molecular Biology & Protein Science Laboratory, Department of Genetic Engineering and Biotechnology, University of Rajshahi, Rajshahi-6205, Bangladesh.
Email: reza.gen@ru.ac.bd

Funding information
University Grants Commission (UGC) Bangladesh, Grant/Award Number: 917-5/52/UGC/Science 9/2015

Nickel is a fundamental element for healthy life for human and higher animals. For biological importance, its complexation with bioactive ligand is worth to be studied with the aim to understand its function. Using mouse peritoneal cancer model, MTT colorimetric assay and anticancer activity analysis, we examined the role of nickel(ll) complex in growth inhibition of cancer cells. A novel nickel(ll) complex was synthesized and characterized using physicochemical and spectroscopic techniques. The study indicated that both the ligand and complex were capable of inhibiting Ehrlich Ascites Carcinoma (EAC) cells growth by 28.21% and 44.52%, respectively, when administered 0.3 mg/kg/day body weight intraperitoneally for five consecutive days in Swiss Webstar mice. Determination the LD_{50} of the complex (55 mg/kg) allowed adjusting the dose as 2.75 mg/kg and upon administration, inhibition increased to 69.36%. The ligand and complex have shown an inhibitory effect in the range of 4.86%–67.3% and 6.1%- 89.37%, respectively, against EAC cells (concentration range of 31.25–500 μg/ml) in RPMI-1640 medium as determined by MTT colorimetric assay. Apoptotic cell morphological alteration was determined through optical and fluorescence microscopy. Up regulation of P^{53}, Bax, Cas-8, Cas-3 and Fas and down regulation of NF-kB and Bcl-2 gene expression were observed in the cells treated with the nickel(ll) complex for five consecutive days. In conclusion, the newly synthesized nickel(ll) complex has shown

Abbreviation: L, Ligand; Ni, Nickel; MTT, 3-[4, 5-dimethylthiazol-2-yl]-2, 5 diphenyl tetrazolium bromide; EAC, Ehrlich Ascites Carcinoma; LD_{50}, Lethal Dose 50%; RPMI-1640, Roswell Park Memorial Institute; PBS, Phosphate Buffered Saline; ONS ligand, Oxygen, Nitrogen, Sulpher ligand; SBDTC, S-benzyl dithiocarbazate; GAPDH, Glyceraldehyde-3-phosphate dehydrogenase; M-MLV, Moloney Murine Leukemia Virus; dNTP, Deoxynucleotide triphosphate; IR, Infra Red; KBr, Potassium Bromide; DMSO, Dimethyl sulfoxide; H_3L, benzyl-3-N-(2,4-dihydroxyphenylmethylene) hydrazine carbodithioate; icddr'b, International Centre for Diarrhoea Disease Research, Bangladesh; IBSc, Institute of Biological Sciences; OD, Optical Density; RT- PCR, Reverse transcriptase polymerase chain reaction; MST, Median Survival Time; %ILS, Percentage increase in life span; SEM, Standard error of mean; HRMS, High Resolution Mass Spectrometer; LRMS, Low Resolution Mass Spectrometer; ALT, Alanine aminotransferase; AST, Aspartate aminotransferase; ALP, Alkaline phosphatase.

anti-proliferative activity and can further be optimized to be used as a lead molecule for anticancer drug.

KEYWORDS

anticancer activity, apoptosis, DNA fragmentation, nickel(ll) complex, ONS ligand

1 | INTRODUCTION

Medicinal inorganic chemistry is one of the quickest developing areas of pharmaceutical research.[1] One of the rudimentary goals in this field is the development of new anticancer and antimicrobial therapeutic agents, which represent an effective strategy towards these pathologies as the metal ions and complexes are able to bind with nucleic acids stereo-specifically with varying strength and specificity.[2] Cobalt, nickel, copper, and zinc are fundamental elements which promote sound health to human and higher animals[3] that is giving consideration to biologically relevant metals attached to various biomolecules to conduct physiological activities. Among these metals, nickel is associated with several enzymes and plays a role in physiological processes as a cofactor in the absorption of iron from the intestine.[4] Any change in its concentration leads to metabolic disorder.[5] Being the nickel of biological importance, its complexation with bioactive ligands is worth to be studied with the aim to understand functions of its complexes and to explore new bioactive compounds.[6,7] The bioinorganic role of nickel and the bioavailability in its dependent enzymes such as in urease, *E. coli* glyoxalase I, [NiFe]-hydrogenase, methyl-CoM reductase, CO dehydrogenase, and acetyl coenzyme A synthase, is widely recognized.[8] The structure of nickel proteins has greatly explored by means of the X-ray crystallography.[9] Many studies traced the role of metal ions in major biological processes. Thus, the inorganic pharmacology initiated to be an essential field with more than 25 inorganic compounds, being used in therapeutic purposes by developing antibacterial, antiviral, and anticancer drugs.[10,11] Kirschner et al. [10] have revealed that the transfer of the metal ion from the ligand to the cancer associated viruses was a principal, mechanism for designing new anticancer drugs. Several *in vivo* researches have been investigated[12] that biologically functional compounds become more bacteriostatic and carcinostatic upon chelation.

Ligands having oxygen and nitrogen as donor atoms are generally studied and the number of chemical studies in this area has been remarkably grown over the years when sulfur donor chelating agent has found.[13] Nowadays these ligand associated complex systems gain immense coverage in diverse areas, ranging from general considerations of the effect of sulfur and electron delocalization in transition metal complexes to potential biological activity and practical purposes.[14–16] In fact modification of platinum(ll) antitumor complexes with sulfur ligands have been described[17] and palladium(ll) compounds with O,S bidentate ligands were tested for their anti-proliferative and pro-apoptotic activities.[18]

The class of thiosemicarbazones, a structural analogue of the thiocarbohydrazone, has been reported to exhibit anticancer activity owing to the specific and unique properties of their metal chelate.[19,20] It was suggested that these compounds, may act by virtue of their chelating potentiality at the cellular level thereby exerting antiproliferation activity.[21] Nickel(ll) ion established superficial and stable complexes of various kind spheres with nitrogen and sulfur donor ligands holding dithiocarbazate molecule based on the ligand precursor constructing the Schiff base.[22] Many nickel(ll) complexes of dithiocarbazate Schiff bases have been studied for their potential biological activities as anticancer, anti-inflammatory and antimicrobial activities.[22,23] However, their mechanistic pathway to exhibit bioactivity still lacks information. For this reason, we have synthesized a four coordinate labile nickel(ll) complex of tridentate ONS Schiff base ligand took from S-benzyl dithiocarbazate (SBDTC) with 2,4-dihydroxy benzaldehyde and examined it's *in vivo* antiproliferative activity along with the apoptotic pathway in mice model.

2 | MATERIALS AND METHODS

2.1 | Chemicals and reagents

Each chemicals and solvents were of reagent grade and used without purification. Hydrazine hydrate (90%), carbon disulfide, potassium hydroxide, and benzyl chloride were purchased from Merck (India), while 2, 4-dihydroxy benzaldehyde, trypan blue and Hoechst 33342 were obtained from Sigma-Aldrich (USA). Nickel(II) acetate tetrahydrate was obtained from FlukaChemica (Switzerland). The solvents acetonitrile, chloroform, dichloromethane, dimethyl sulfoxide, ethanol, methanol and toluene were also purchased from Active Fine Chemicals Ltd (Bangladesh). M-MLV reverse transcriptase, dNTPs and oligo (dT), GAPDH, p53, Bax, Bcl-2, caspase-3, caspase-8, NFkB and Fas were obtained from Tiangen Biotech, Beijing, China.

2.2 | Instrumentation

IR spectra (4000–400 cm^{-1}) were taken as KBr pellets using an IR Affinity 1S spectrophotometer (Shimadzu, Kyoto, Japan). Magnetic susceptibility and molar conductance measurements were made on a magnetic susceptibility balance Sherwood Scientific (Cambridge, UK) and an ECOSCAN CON5 conductivity/temperature meter (Eutech Instruments, Singapore). UV–vis spectra were recorded on a T60 UV–vis spectrophotometer (PG Instruments, UK) programmed with Win5 software, version 5.1, between 200–1100 nm using 10^{-3} M solution in DMSO. On the other hand, mass spectra (m/z: 0–1200) were obtained on a JEOL-JMS-D300 mass spectrometer.

2.3 | X-ray crystal structure determination

Intensity measurements for the structure reported were carried out at 173(1) K on a Rigaku R-AXIS RAPID diffractometer using filtered Mo-K_λ radiation (λ = 0.71075 Å). The structure was solved by direct methods[24] and successive Fourier syntheses. The hydrogen atoms were integrated at deliberated positions and constrained to ride on the atoms to which they are attached. The phenyl moiety showed a positional disorder and two orientations each at half occupancy of the ring were successfully refined. The entire calculations were executed using the Crystal Structure package,[25] except for refinement for which the full-matrix least-squares method based on F^2 with all observed reflections was used.[26]

2.4 | Synthesis of the Schiff base H_3L

The benzyl-3-N-(2,4-dihydroxyphenylmethylene) hydrazine carbodithioate (H_3L) was prepared at it follows: a solution of 2,4-dihydroxybenzaldehyde (0.414 g, 3 mmol) in ethanol (5 ml) was added to a boiling solution of S-benzyl dithiocarbazate (0.594 g, 3 mmol) in ethanol (15 ml) and the aliquot was refluxed for 1 hr. The resulting yellow solution was allowed to stand at 5°C in a refrigerator for two days. The light yellow precipitate, which formed was separated by filtration, washed with ethanol and dried in vacuum over anhydrous $CaCl_2$.

Selected IR bands ν (cm^{-1}): 3329 strong and broad (O-H, phenol, hydrogen bonded), 3101 s (N-H), 2972, 2864 s (C-H, -CH_2), 1635 vs (C=N), 1576 m, 1506 m (C=C), 1462 m (C-H, -CH_2, bend), 1217s (C-O, phenol), 1340 m (O-H, in plane bending), 1101 m (C=S), 1028 s (N-N), 977 m (CSS), 856, 839 w (C-H, OOP, *p*-disubstitution), 694 m (C-H, OOP, *o*-disubstitution). UV–vis spectrum [λ_{max}, DMSO, nm ($Lmol^{-1}$ cm^{-1}): 295 (3.39), 325 (3.29), 350 (3.27), 365 (3.23), 395 (3.22). LRMS (FAB, 70 eV, %) m/z: 319 for $C_{15}H_{14}N_2O_2S_2$ as (M^+, 53.68%), 195 (M-$C_6H_5CH_2S$, 25.26%), 154 (M-($C_6H_5CH_2S$ + N_2CH), 100%), 136 (M-($C_6H_5CH_2S$ + N_2CH+ OH)), 71.05%), 107 (M-($C_6H_5CH_2S$ + N_2CH + OH + S)), 16.58%), 91 (M-($C_6H_5CH_2S$ + N_2CH + OH + S + O)), 31.18%), 39 (M-($C_6H_5CH_2S$ + N_2CH + OH + S + O + C_4H_4)), 6.32%). HRMS for $C_{15}H_{15}$ $N_2O_2S_2$ (m/z): 319.0574, 75.40).

2.5 | Synthesis of the nickel(II) complex

The complex [acetonitrile-benzyl-3-*N*-(2,4-dihydroxyphenylmethylene)hydrazinecarbodithioato-κ^3-N′,S,O] nickel(II), [Ni (HL)CH_3CN], was prepared *in situ* subsequently the formation of the Schiff base. A mixture of 2,4-dihydroxy benzaldehyde (0.276 g, 2 mmol) in ethanol (10 ml) and SBDTC (0.396 g, 2 mmol) in hot ethanol (30 ml) was refluxed for 1 hr. Then nickel(II) acetate tetrahydrate (0.248 g, 1 mmol) in ethanol (25 ml) was added to the resultant yellow solution and reflux was continued for further half an hour. The brown precipitate which formed was separated by filtration, washed with hot ethanol and dried in vacuum over anhydrous $CaCl_2$. Selected IR bands ν (cm^{-1}): 3198–3364 strong and broad (O-H, phenol, hydrogen bonded), 2914, 2783 m (C-H, -CH_2), 1622 s, 1537s (C=N), 1583 m, 1435 m (C=C), 1465 m (C-H, -CH_2, bend), 1250 s (C-O, phenol), 1361 m (O-H, in plane bending), 1068 w (N-N), 977 m (CSS), 848 w (C-H, OOP, *p*-disubstitution), 700 w (C-H, OOP, *o*-disubstitution), 495 mw (M-N), 418 w (M-S). UV–vis spectrum [λ_{max}, DMSO, nm ($Lmol^{-1}$ cm^{-1}): 295 (3.40), 325 (3.29), 350 (3.27), 363 (3.22), 395 (3.23), 430 (3.28), 690–795 (1.28). LRMS (FAB, 70 eV, %) m/z: 459 for $C_{17}{}^1H_{12}{}^2H_6N_2O_3S_3Ni$ as (M^+, 1.96%), 375 (M-(DMSO-d_6), 1.65%), 322 (M-(DMSO-d_6 + Ni)), 1.68%); 290 (M-(DMSO-d_6 + Ni + O_2)), 2.68%); 238 (M-(DMSO-d_6 + Ni + O_2 + 4C)), 9.47%); 169 (M-(DMSO-d_6 + Ni + O_2 + 4C + $C_3H_5N_2$)), 80.52%); 137 (M-(DMSO-d_6 + Ni + O_2 + 4C + $C_3H_5N_2$ + S)), 14.84%); 86 (M-(DMSO-d_6 + Ni + O_2 + 4C + $C_3H_5N_2$ + C_4H_4)), 100%); HRMS for $C_{17}{}^1H_{13}{}^2H_6N_2O_3S_3Ni$ (m/z): 459.0292, 6.87%).

2.6 | Animal use and ethical clearance

Adult male\female Swiss Webstar mice, 6–8 weeks old (25 ± 4 g body weight), were collected from the animal resource branch of the International Centre for Diarrhoea Disease Research, Bangladesh (icddr'b). Experimental mice were accommodated in polypropylene cages containing clean wood chips as bedding materials. Maximum six mice per cage were maintained with controlled conditions (12:12 hr light–dark with temperature 22 ± 5°C) along with utmost hygiene. They were maintained under conditions. Institute of Biological Sciences (IBSc),

University of Rajshahi, Bangladesh approved ethical clearance (license no: 225/320-IAMEBBC/IBSc).

2.7 | Acute toxicity study

The acute oral toxicity of metal complex in male Swiss Webstar mice was studied as per reported method.[27]

2.8 | Hemolytic activity test

The Hemolysis assay was done as stated by Henkelman et al.,[28] In brief, 5 ml of blood were collected from goat in tubes containing 3.8% trisodium citrate as anticoagulant and spined at 5000 rpm for 20 min. The supernatant was fully discarded by aspiration with highest care using micropipette and afterwards the blood cells were washed 3 more times with 0.9% NaCl at 5000 rpm for 15 min to prepare 10% RBC in 0.9% NaCl. 150 μL of 10% RBC suspension were mixed with 25, 50, 100 μL of test samples (10 mg/ml); 1350 μL of 0.9% NaCl were used as negative control (Blank) and 1350 μL of dH_2O as positive controls. Reaction mixture was incubated at 37°C in a water bath for 60 min. The volume of the reaction mixture was diluted to 1.5 ml by adding 0.9% NaCl. Finally it was centrifuged at 3000 rpm for 5 min and the resultant hemoglobin concentration in the supernatant was spectrophotometrically measured at 540 nm.

The percentage hemolysis was calculated as follows:

% Hemolytic activity = [Sample OD/H_2O OD] x 100.

2.9 | Cell culture

Ehrlich ascites carcinoma (EAC) cells were purchased by the courtesy of the Indian Institute of Chemical Biology, Kolkata, India. The cells were maintained as mammary gland cancer cell in ascites in Swiss webstar mice by intraperitoneal inoculation (biweekly) of 1×10^6 cells/mouse. For *in vitro* study, EAC cells were cultured in the RPMI - 1640 (Roswell Park Memorial Institute) medium having glucose 2 mM, L-glutamine in presence of 10% fetal calf serum, and 1% (v/v) penicillin–streptomycin in a humidified atmosphere of 5% CO_2 at 37°C.

2.10 | MTT colorimetric assay

Cytotoxicity of ligand and its nickel(ll) complex against EAC cell was assayed by MTT (3-[4, 5-dimethylthiazol-2-yl]-2, 5 diphenyl tetrazolium bromide) colorimetric technique.[29] For this experiment, 1×10^6 EAC cells in 200 μL RPMI-1640 media were taken each well of in a 96-well plate., Five serially diluted concentrations (500, 250, 125, 62.5, and 31.25 μg/ml) of ligand and of complex were used into each well of EAC cells to evaluate highest efficacy. EAC cells treated solvent with DMSO was used as control. By conducting the assay in triplicate the experimental error was reduced.

CO_2 incubator with 80% humidity was applied to incubate EAC cells for 24 hr at 37°C. Later, aliquots from each well were removed and 180 μL of phosphate buffered saline (PBS) and 20 μL (5 mg/ml in PBS) of MTT were added into each well. The plates were then placed into a dark place at 37°C for 8 hr to allow the reaction, After the aspiration of aliquots from each wells 200 μL of acidic isopropanol (0.1 N HCl in absolute isopropanol) were added followed by incubated at 37°C for 1 hr. Finally, absorbance was taken at 570 nm in microtiter plate reader (Optica Microplate Reader, Mikura Ltd., Horsham, UK) to calculate the cell proliferation inhibition ratio (%) was calculated as (A − B) × 100/A, where, A and B are the optical density (OD) at 570 nm of the cellular homogenate without and in presence of metal complex, respectively.

2.11 | *In vivo* cell growth inhibition

To evaluate the cell growth inhibition of the ligand and complex, five groups of Swiss webstar mice ($n = 6$) weighing 25 ± 4 g were used.[30] Around 1×10^6 EAC cells were interperitonially inoculated into each mice from all groups of on day 0. Treatments started after 24 hr of tumor inoculation and continued for 5 days. Groups 1 and 2 received ligand and its nickel(ll) complex at the doses of 0.3 mg/kg/day and group 3 received metal complex at the dose of 2.75 mg/kg/day (dose selected after LD_{50} determination), via intraperitoneal injection. Group 4 received the anticancer drug bleomycin (0.3 mg/kg/day); whereas group 5 was used as control receiving 10% DMSO only. Mice of each group were sacrificed the sixth day and the total intraperitoneal cancer cells were harvested by 0.98% normal saline. Viable cells were first identified with trypen blue and then counted by a hemocytometer under inverted microscope (XDS-1R, Optika, Bergamo, Italy).

Cell growth inhibition was calculated by the following formula:

% Cell growth inhibition = (1 − T/C) × 100.

(Where T = mean number of tumor cells of treatment group and C = mean number of tumor cells of control group).

2.12 | Cell Morphology and nuclear damage Study by Optical and Fluorescence Microscopy

Morphological observation of EAC cells in both treated (0.3 mg/kg/day) and control groups were carried out using an optical and fluorescence microscope (Olympus

IX71, Seoul, Korea).[31] In short, EAC cells were harvested from the experimental mice and stained with 0.1 μg/ml of Hoechst 33342 at 37°C for 20 min in dark. Then the EAC cells were washed and resuspended in PBS to observe the morphological alterations which were analyzed using optical and fluorescence microscopy.

2.13 | DNA fragmentation assay

DNA fragmentation in treated cells was determined using the previously described method.[32] EAC cells were collected from both treated (five consecutive days at 2.75 mg/kg/day) and control (no treatment) mice. The total DNA was isolated from the cells by using a kit (Promega, Madison, WI, USA) and analyzed by electrophoresis on 1% agarose gel containing 0.1 μg/ml ethidium bromide (EtBr) to visualize in gel documentation system (AlphaImager ® Mini System, Protein Simple).

2.14 | Total RNA isolation and cDNA preparation

Total RNA was extracted using RNAsimple RNA isolation kit (Tiangen, Beijing, China) according to the protocol provided with the kit. Absorbances of the isolated RNA was measured at 260 and 280 nm using nanodrop 2000 spectrophotometer (Thermo scientific) to assess the concentration and purity. 3 μg of isolated RNA was converted to cDNA using 2 μL oligo (dT), 1 μL M-MLV reverse transcriptase, 2 μL dNTPs, 4 μl 5× 1st strand buffer and required amount of dH_2O in a total volume of 20 μl rxn mixture.

2.15 | Reverse transcriptase polymerase chain reaction (RT- PCR)

The expression levels of GAPDH, p53, Bax, Bcl-2, Cas-3, Cas-8, Fas and NFκB, RT-PCR were done as previously described.[33] In brief, the first-strand cDNA was amplified by polymerase chain reaction using gene specific oligoes. 25 μL reaction volumes were prepared containing 1X Taq polymerase buffer, 25 pmol each of forwarded and reverse primers, 2.5 mM of each dNTPs and 0.25 μL of platinum Taq polymerase (Tiangen, China). The subsequent specific oligonucleotides (IDT, Singapore) were used.

GAPDH upstream-(5'-GTGGAAGGACTCATGACCA CAG-3′) and downstream-(5'-CTGGTGCTCAGTGTAG CCCAG-3′) generating a band of 350 bp; *p53* upstream-(5'-GCGTCTTAGAGACAGTTGCCT-3′) and downstream-(5'-GGATAGGTCGGCGGTTCATGC-3′) generating a band of 500 bp; *Bax* upstream-(5'-GGCCCACCAGCTCTGAGCA GA-3′) and downstream-(5'-GCCACGTGGGCGTCCC AAAGT-3′) generating a band of 500 bp; and 350 bp; *Bcl-2* upstream-(5'-GTGGAGGAGCTCTTCAGGGA-3′) and downstream-(5'-AGGCACCCAGGGTGATGCAA-3′) generating a band of 150 bp; *NFkB* upstream-(5'-AACAAAATGCCCCACGGTTA-3′) and downstream-(5'-GGGACGATGCAATGGACTGT-3′) generating a band of 125 bp; *Cas-8* upstream-(5'-TCGCCTCGAGGACATCGCT CTC-3′) and downstream-(5'-CTGCTGGGGATGGCCA CTGTG-3′) generating a band of 600 bp and 350 bp; *Cas-3* upstream-(5'-TTAGTGATAAAAATAGAGTTCTTT TGT-3′) and downstream-(5'-TTAATAAAGGTATCCA TGGAGAACACT-3′) generating a band of 450 bp and 250 bp; *Fas* upstream-(5′-AGCTTGGTCTAGAGTG AAAA-3′) and downstream-(5′- GAGGCAGAATCATG AGATAT-3′) generating a band of 900 bp and 200 bp.

The thermal cycler (Gene Atlas 482, Japan) program for amplification reactions was set at 95°C for 3 min, 95°C for 1 min and 52–58°C for 1 min (variable annealing temperature for different gene product) 35 cycles followed by 72°C for 1 min, 72°C for 10 min and eventually hold at 20°C. Expression of the mRNA of a housekeeping gene GAPDH was analyzed to measure the relative expression of the different genes. The PCR products of these genes and GAPDH were electrophoresis in 1% agarose gel with EtBr staining to visualize under UV-trans illuminator (Protein simple).

2.16 | Determination of Median Survival Time and Percentage increase in life span

The mean survival period of the EAC-bearing mice was inspected by previously described methods[34] which was applied to the five assigned groups of mice consisting 6 mice per group. For therapeutic assessment, 1×10^6 EAC cells/mouse were inoculated to each one group of mice on day 0. Treatment in progress after 24 hr of tumor inoculation and continued until death. Group 1 was treated with bleomycin; groups 2–3 received Ni complex at different concentrations; group 4 received ligand (H_3L) and animals of group 5 used as solvent (10% DMSO) control. The survival time of the mice in each group was recorded and the mean value of survival time (in days) of each group was calculated.

$$\%\text{ILS} = \frac{\text{Mean survival time of the treated group}}{\text{Mean survival time of the control group}} - 1 \times 100$$

$$\text{Mean survival} = \text{Day of 1st death} + \text{Day of last death}/2$$

2.17 | Hematological parameters

The haematological parameters (WBC, RBC and Hb content) were determined by standard methods as previously

described.[34] Total WBC and RBC were counted by microscope with a haemocytometer, and the percentage of hemoglobin (%Hb) was measured by hematometer.

2.18 | Liver and kidney function test

To study the liver function of treated group in comparison with control, the amount of ALT, AST, ALP and total Bilirubin, were determined by enzymatic (NADH without P-S′-P) and traditional method (diazo reaction), by means of the Abbot Architect Plus $C_{i\ 4100}$ (bilirubin, ALT, AST) and Siemens Dimension RL Max (ALP) instruments. In brief, blood was collected by the cardiac puncture of each group on the 6th day of EAC-cell inoculation, centrifuged at 4000 rpm for 10 min. and serum was taken and preserved at −20°C or used instantly.

To evaluate the kidney function, urea and creatinine, were measured by enzymatic (urease) Jaffe (alkaline picrate) method by using the Abbot Architect Plus $C_{i\ 4100}$instrument. The sample collection and preservation was done likewise discussed above.

2.19 | Histopathology

The major organs like liver and kidney were collected from the experimental (dose: 0.3 mg/kg bwt) animals (on day 6th) and processed by standard protocol[35] to prepare tissue slides by hematoxylin and eosin staining. The slides were observed under Motic Advanced system microscope (B, series) with the help of Motic J1.0 software in a Macintosh computer.

2.20 | Statistical analysis

Experimental data were taken with considerable replication (triplicate). All data were expressed as mean ± SEM. Significance test was carried out between the control and treatment by one-way ANOVA followed by Dunnett post hoc test using SPSS 16 software. Significance was tested at 5%, 1% and 0.1% level (where p* value 0.05, p** value 0.01 and p*** value 0.001, respectively).

3 | RESULTS

3.1 | Melting point and % of Yield

For ligand; light yellow prismatic single crystals were obtained from a mixture of ethanol and acetone (2:1; v/v) after 15 days and the % of yield 77 (0.782 g). Its melting point was 186–188°C. For nickel(ll) complex; needle shaped brownish single crystals were isolated in acetonitrile at room temperature and the % of yield 45(0.412 g) where its melting point was 278–280°C (d).

3.2 | Spectroscopic characterization

The ligand (H_3L) as KBr disc exhibited a very strong band at 1635 cm^{-1} for the ν (C=N), stretching vibration, which shifted to 1622 cm^{-1} in its nickel(II) complex, suggesting the coordination through the azomethine nitrogen atom (>CH=N).[19,36] Generally the dithiocarbazate Schiff bases may exist in thiol [>N-N=C (SH)-SR] or thione [>N-NH-C(=S)-SR] tautomeric form.[23] However, the presence of the ν (C=S) strong band at 1101 cm^{-1} and the absence of the ν (S-H) band in the free ligand indicated that the Schiff base exists predominantly in its thione (>C=S) form in the solid state and the absence of this band in the nickel(II) complex indicated the involvement of thione sulfur (>C=S) in coordination in its deprotonated thiol form (>C-S^-). This is also supported by the increase of the ν (N-N) stretching from 1028 cm^{-1}(in the free ligand) to 1068 cm^{-1} in the complex. Additionally, the free ligand showed a strong and broad absorption at 3329 cm^{-1} due to the hydrogen bond ν (O-H) stretching, which was observed in the complex as broad absorption band in the region 3364–3198 cm^{-1}.

The solution electronic spectrum of the Schiff base in DMSO showed bands at 295, 325, 350, 365 and 395 nm, tentatively assigned to the $\pi \rightarrow \pi^*$ (ring), $\pi \rightarrow \pi^*$ (CH=N), $n \rightarrow \pi^*$ (CH=N), $\pi \rightarrow \pi^*$ (dithiocarbazate) and $n \rightarrow \pi^*$ (dithiocarbazate) transitions, respectively.[23,37,38] The presence of $\pi \rightarrow \pi^*$ (dithiocarbazate) band also supported the existence of the thione tautomeric form in the free ligand. Although the bands at 295 and 395 nm are prominent, the remaining bands are very close to each other and appeared as shoulder in between the $\pi \rightarrow \pi^*$ (ring) and $n \rightarrow \pi^*$ (dithiocarbazate) transitions both in the free ligand and its complex. In addition to these intraligand transitions, the complex showed a strong absorption band at 430 nm for the S → Ni, which is basically charge transfer in nature. Moreover, the complex also showed a very week broad band in the region 690–795 nm for the d-d transition, diagnostic to the square-planar nickel(II) as supported by the diamagnetic behavior of the complex.[37,38]

The low resolution mass spectrum of the Schiff base showed a molecular ion peak at m/z 319 that supported the fragment ion peaks at m/z of 195, 154, 137, 105, 91 and 39 due to the successive loss of $C_6H_5CH_2S$, N_2CH, OH, S, O and C_4H_4, respectively from the molecule. A molecular ion peak at m/z 319.0574 in its high resolution mass spectroscopy confirmed the proposed structure of the ligand. However, an interesting phenomenon was observed in the low resolution mass spectrum of the complex in DMSO-d_6. As discussed in the crystallographic part of this section, the molecular weight of the complex was determined as 416.14 g/mol, indicating the formation

of a four coordinate monochelated complex containing an acetonitrile molecule as co-ligand. The mass spectrum molecular ion peak at m/z of 459 in the complex evidenced the substitution of acetonitrile ligand with the more coordinating solvent molecule DMSO. The molecular ion peak was also confirmed by HRMS analysis of the complex. The complex formulation was also supported by fragment ions observed at m/z 375, 322, 290 etc., because of successive removal of DMSO, Ni and O_2, respectively, from the molecule.

3.3 | Crystal structure of [Ni (HL)CH_3CN] complex

The molecular and crystal structure of the [Ni (HL)CH_3CN] complex was determined by single-crystal X-ray diffraction analysis. An ORTEP drawing of the complex with the atom numbering scheme is shown in Figure 1a. The complex crystallizes in orthorhombic system with space group $P\text{na}2_1$. The crystal structure shows that the complex adopts a four coordinate configuration with the Schiff base coordinated to the nickel(ll) ion in its deprotonated form as a dinegative tridentate ONS chelating agent via its thiolate sulfur, azomethine nitrogen and phenolate oxygen atoms as observed in other orthohydroxy benzaldehyde Schiff bases of S-benzyldithiocarbazate (SBDTC) or S-methyldithiocarbazate (SMDTC).[38–42] The fourth coordination site in the square planar geometry of the nickel(ll) ion is occupied by a nitrogen atom of acetonitrile molecule used as solvent during crystallization. Crystal data and details of refinement of the nickel(ll) complex are summarized in Table 1, while selected bond lengths and angles for the title complex are reported in Table 2. The Ni-S(1), Ni-N(1), Ni-O(2) bond lengths of chelating ligand are of 2.1439(11), 1.842(2) and 1.846(2) Å, respectively, comparable to related mixed ligand four coordinate nickel(ll) complexes of oxyphenyl dithiocarbazate Schiff bases (Table 3).[38–41] On the other hand the Ni-S(1) and Ni-N(1) bond lengths are significantly shorter than those measured in bischelated octahedral Ni-pyridyl methylenedithiocarbazate complexes (range of 2.3952(6)- 2.4257(6) and 1.9961(18)- 2.0000(18) Å,

TABLE 1 Crystallographic data of [Ni (HL)CH_3CN] complex

Empirical formula	$C_{17}H_{15}N_3NiO_2S_2$
Fw	416.14
Crystal system	Orthorhombic
Space group	$P\text{na}2_1$
a, Å	12.8279(5)
b, Å	26.4885(11)
c, Å	5.1981(2)
V, Å^3	1766.27(13)
Z	4
*D*calcd, g cm^{-3}	1.565
Crystal size, mm	0.420 × 0.130 × 0.060
μ (Mo-Kα), mm^{-1}	1.350
F(000)	856.00
θmax, deg	25.32
No. of reflections collected	13842
*R*int	0.0546
T_{min}, T_{max}	0.556, 0.922
No. of independent reflections	3225
No. of observed reflections ($I > 2\sigma(I)$)	2927
No. of refined parameters	273
goodness-of-fit, *S* (F^2)	1.141
*R*1, *wR*2 ($I > 2\sigma(I)$)	0.0348, 0.0808
residuals, e/Å^3	0.54, −0.24

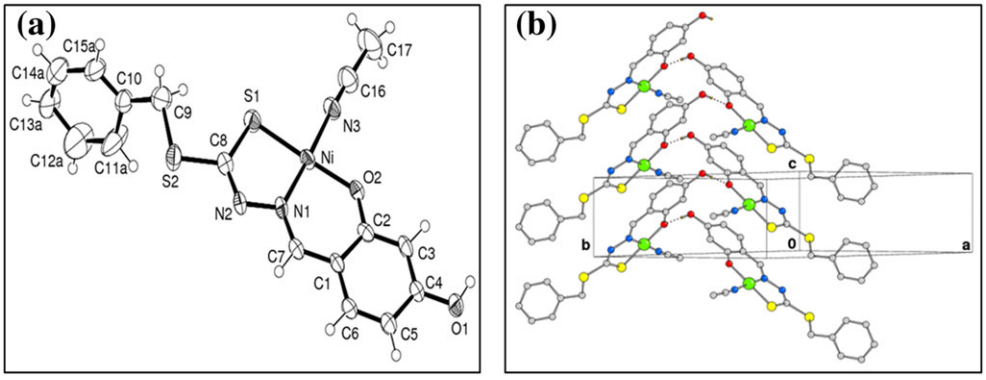

FIGURE 1 Structural illustration of the [Ni (HL)CH3CN] complex. (a) Thermal ellipsoids at 50% probability level (ORTEP diagram) of the [Ni (HL)CH_3CN] complex. Of the disordered phenyl group (see exp. section) only one orientation is displayed. (b) Crystal packing diagram for the [Ni (HL)CH_3CN] complex showing the herringbone arrangement of complexes connected by O(1)-H ... O(2) hydrogen bond shown as dashed line (Only H atom at O1 is shown)

TABLE 2 Selected bond distances (Å) and bond angles (°) for [Ni (HL)CH_3CN] complex

Ni-S(1)	2.1439(11)	N(1)-Ni-O(2)	95.25(11)
Ni-N(1)	1.842(2)	N(3)-Ni-S(1)	89.35(10)
Ni-O(2)	1.862(2)	N(1)-Ni-S(1)	87.95(9)
Ni-N(3)	1.878(3)	N(3)-Ni-O(2)	87.45(11)
S(1)-C(8)	1.732(3)	N(1)-Ni-N(3)	177.30(13)
S(2)-C(8)	1.763(3)	S(1)-Ni-O(2)	176.57(7)
S(2)-C(9)	1.816(5)	C(2)-O(2)-Ni	127.6(18)
C(8)-N(2)	1.278(5)	C(8)-S(1)-Ni	95.36(13)
C(7)-N(1)	1.295(5)	C(8)-N(2)-N(1)	112.1(2)
N(1)-N(2)	1.424(3)	N(2)-N(1)-Ni	120.9(2)

respectively).[20] Variability in coordination distances are commonly observed in these types of nickel(ll) complexes, depending on the structure and denticity of the ligands used.[43,44]

The coordination sphere is accomplished by an acetonitrile molecule bound at nickel (Ni-N(3)) with a bond length of 1.878(3) Å. The coordination bond angles (Table 1) are very close to a regular square-planar geometry (not exceeding deviations larger than 6°), indicating no particular strain in the coordination sphere. The N(1)-N(2) and C(8)-S(1) bond lengths of 1.424(3) and 1.732(3) Å respectively, suggest their single bond character.[23,39]

The crystal packing evidences the [Ni (HL)CH_3CN] complex connected by an hydrogen bond realized between O(1)-H and oxygen O(2) of a symmetry related complex {O(1) .... O(2) = 2.746(3) Å, O(1)-H .... O(2) = 1.91 Å, O(1)-H ... O(2) angle = 172° forming an herringbone polymeric arrangement developed in the direction of axis *c* as shown in Figure 1b. On the other hand no appreciable π-π interaction among aromatic rings is present in the crystal packing.

3.4 | Acute toxicity study

The acute toxicity studies mainly aim to establish the therapeutic index (the ratio between the pharmacologically effective dose and the lethal dose on the same strain and species). The nickel(ll) complex showed toxicity at a dose of 55 mg/kg (i.p.) body weight. The behavior of the animals was observed for the first 3 h, then at intervals of 4 h during the next 24 hr. The complex caused mortality in mice during 24 h, but little behavioral changes were observed. Food and water intake revealed no significant difference among the group studied.

3.5 | Hemolytic activity test

Some of study reveals that human erythrocytes membranes from blood types show different stability as determined from the mean corpuscular fragility.[28] Chemical agent can positively affect the red cell membrane[45] and on the contrary many of them have severe undesirable effects, which induce hemolytic anemia. For this reason, compounds likely to be used as drug require to be studied for their potential hemolytic activity. The hemolytic activity of the ligand and nickel(ll) complex was evaluated at concentrations ranging from 250–1000 μg/ml (Table 4). It was observed that ligand induced hemolysis (54%–78%), while its nickel(ll) complex induced negligible % hemolysis, which implies that the complex has no potent hemolytic activity.

3.6 | MTT colorimetric assay

The cytotoxic effect of the nickel(ll) complex on EAC cell was assessed by MTT colorimetric assay. The ligand and nickel(ll) complex inhibit cancer cell growth in a dose-dependent manner (Figure 2a and b). Complex showed maximum cancer cell growth inhibition (89.37%) at the concentration of 500 μg/ml. The minimum suppression of

TABLE 3 Comparison of coordination distances (Å) in square-planar nickel(II) complexes with different oxyphenyldithiocarbazato (ONS) ligands

Compound	Ni-S(1)	Ni-N(1)	Ni-O(1)	Ni-X	X	Ref.
[Ni (HL)CH3CN]	2.144(1)	1.842(2)	1.862(2)	1.878(3)	N	This work
[Ni (L1)CN]	2.121(3)	1.859(7)	1.857(6)	1.877(9)	C	[40]
[Ni (Ap-SMe)py]	2.149(2)	1.876(6)	1.827(5)	1.936(6)	N	[39]
{[Ni (L2)Imidazole]	2.149(2)	1.860(5)	1.853(5)	1.923(5)	N	[38]
	2.137(2)	1.865(5)	1.837(5)	1.915(5)	N	
[Ni (L3)PPh3]	2.1451(7)	1.9019(19)	1.8247(17)	2.2177(2)	P	[41]

L^1 = N-methyl-S-methyl-N-(2-hydroxyphenylmethylene)dithiocarbazato

Ap-SMe = 2-Hydroxyacetophenone S-methyldithiocarbazato-

L^2 = Allyl 2-benzylidene-hydrazinecarbodithioate

L^3 = Methyl (1-(2-oxyphenyl)ethylidene)carbonodithiohydrazonato

TABLE 4 Hemolytic assay of ligand (L) and nickel(ll) complex (Ni)

Concentration (μg/mL)	Absorbance at 540 nm	% Hemolysis
Negative control	0.045	0
Positive control	0.478	95.35
L, 250	0.259	54
L, 500	0.339	70
L, 1000	0.375	78
Ni, 250	0.015	3.13
Ni, 500	0.016	3.34
Ni, 1000	0.028	5.85

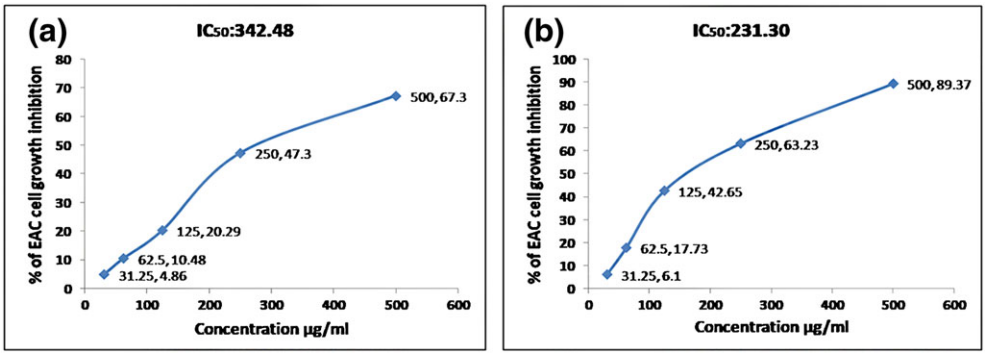

FIGURE 2 *In vitro* cell growth inhibition along with IC_{50}value of Ligand (L) and nickel(ll) complex (Ni) by MTT colorimetric assay. EAC cell growth inhibition was evaluated as dose dependent manner where IC_{50} values were calculated from the dose–response curve. The EAC cells were treated at different doses of (a) L and (b) nickel(ll) complex for 24 hr in RPMI-1640 medium to evaluate the EAC cells growth inhibition

cancer cell growth (6.1%) was observed at 31.25 μg/ml. The IC_{50} value of the ligand and complex was determined as 342.48 and 231.30 μg/mL against EAC cell, respectively.

3.7 | *In vivo* cell growth inhibition

In Table 5, the effects of ligand, complex and bleomycin (standard drug) on EAC cells growth after inoculation are shown and treatment with ligand and complex resulted in significant inhibition of cell growth *in vivo*. The maximum cell growth inhibition with complex was noted at dose of 2.75 mg/kg b.wt/day (69.36%) compared with the control mice where the bleomycin treated mice showed cell growth inhibition by 79.64% (0.3 mg/kg/day).

3.8 | Ligand and complex induced morphological changes and nuclear damage

Morphological changes of EAC cells were examined by Hoechst 33342 fluorescent staining after collecting the cells from mice treated with ligand and nickel(ll) complex

TABLE 5 Effect of ligand (L) and nickel(ll) complex (Ni) on EAC cell growth inhibition in mice

Group	Treatment and Dose (mg/kg b.wt/day)	Viable EAC cell on day 5 after inoculation (x 10^6 cells/ml)	% of cell growth inhibition
1	EAC + Control	280 ± 63.01	
2	EAC + Bleomycin (0.3)	57 ± 0.95*	79.64
3	EAC + L (0.3)	201.33 ± 84.5*	28.21
4	EAC + Ni (0.3)	155.33 ± 43.72*	44.52
5	EAC + Ni (2.75)	85.79 ± 0.57*	69.36

L and Ni inhibit the growth of EAC cells in mice. EAC-bearing mice were treated with L, 0.3 mg/kg/day and Ni, at 0.3 and 2.75 mg/kg/day of concentrations. Data are expressed in mean ± SEM at significant value of $^*p < 0.05$ ($n = 6$) and compared with control.

(0.3 mg/kg/day) for 5 days. Nuclei of EAC cells were round, regular, and homogeneously stained with Hoechst 33342 in control group (solvent treated) as shown in Figure 3a-b. Ligand and complex-treated EAC cells manifested fragmented DNA in nuclei (Figure 3c-d and Figure 3e-f). Chromosome condensation and apoptotic body formation (apoptotic morphologic changes) were also noted in ligand and complex-treated EAC cells. These results indicated that complex treatment could induce apoptosis in EAC cells.

3.9 | DNA fragmentation assay

The activation of the endogenous Ca^{2+}/Mg^{2+}-dependent endonuclease is the most distinctive biochemical hallmark of apoptosis.[32] This activated endonuclease will mediate the cleavage of internucleosomes and generate oligonucleotide fragments. DNA isolated from complex treated EAC cells showed ladder-type DNA that is a characteristic feature of apoptosis induction (Figure 4a).

3.10 | Altered expressions of cancer-related genes in complex-treated cells

Reverse transcription PCR was used to study the mRNA expression levels of several tumor-related genes (Figure 4) in control and complex treated EAC cells (dose of 2.75 mg/kg bwt). The EAC control cells showed high expressions of Bcl-2 and NFkB genes and low expression of Bax genes. A reverse result was observed for EAC cells treated with complex, showing reduced Bcl-2 and NFkB mRNA expressions, whereas the expression level of Bax significantly increased. In addition, the p53, Cas-3, Cas-8 and Fas genes showed increased expressions in complex-treated cells. On the other hand, no or low expression of these genes was seen in EAC control cells.

3.11 | Apoptotic pathway

Using all experimental data specially gene expression and DNA fragmentation, we constructed (Figure 5) an apoptotic pathway of cancer cell growth inhibition by our newly

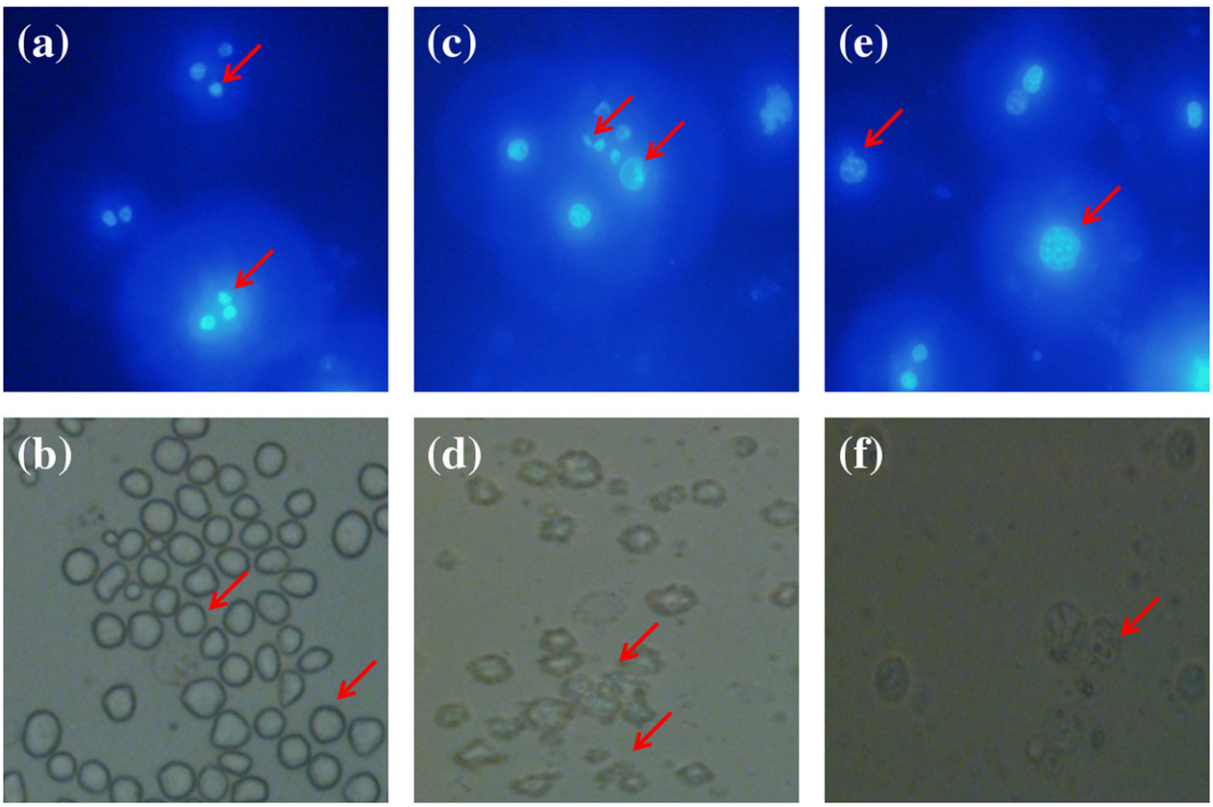

FIGURE 3 Morphological alteration of the Ligand (L) and nickel(ll) complex (Ni) treated EAC cells on fluorescence and optical microscopy. Regular uniform shape of the cells was found in control (untreated mice) in figure (a) (fluorescence microscope) and (b) (optical microscope). Ni treated EAC cells stained with Hoechst 33342 in figure (c) (fluorescence microscopy) and (d) (optical microscope) showed apoptotic features such as chromatin condensation and apoptotic body formation indicated by arrows. L treated EAC cells demonstrate the similar changes were observed in (e) (fluorescence microscopy) and (f) (optical microscope), which were indicated by arrows. (a-f magnification: 25x)

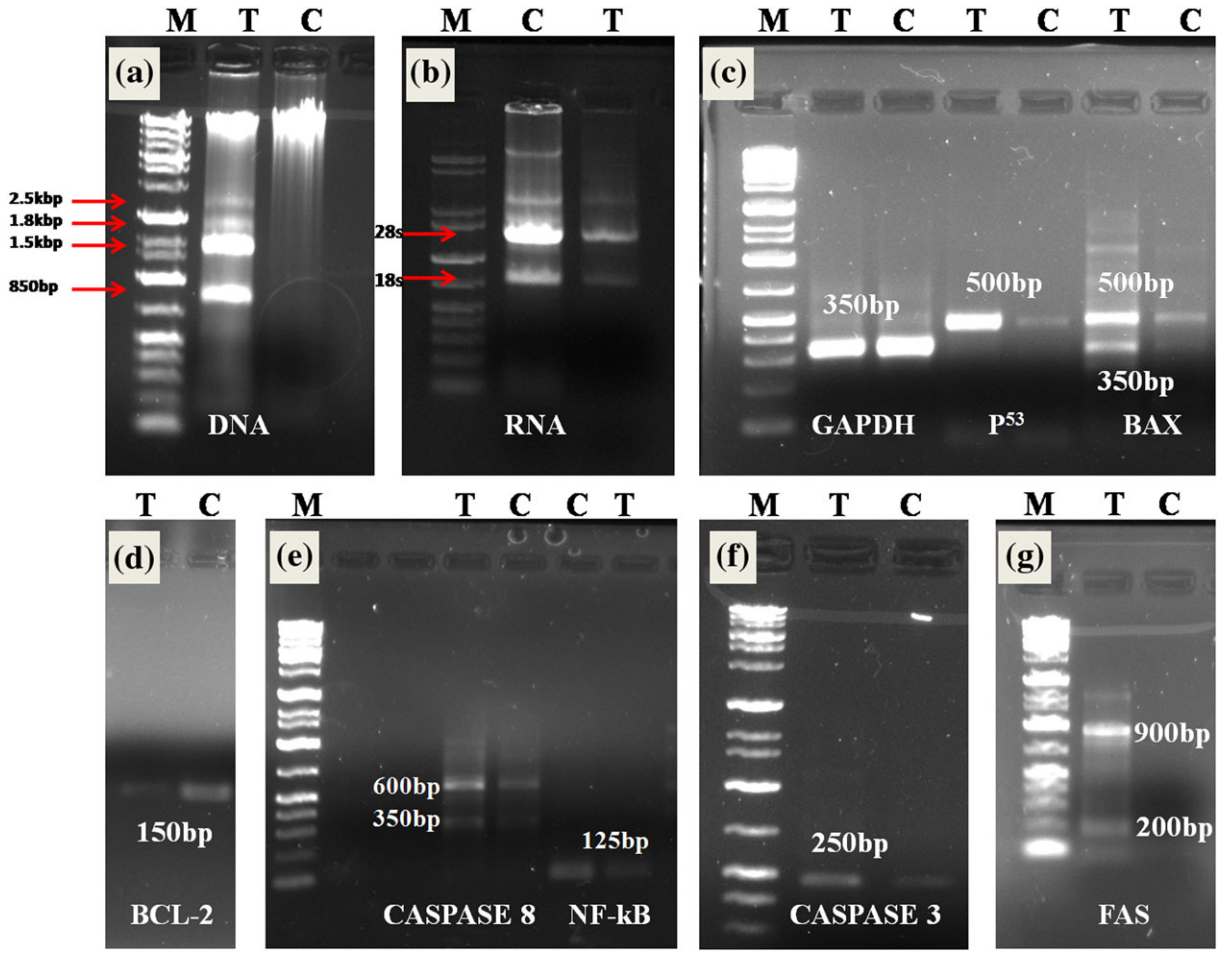

FIGURE 4 Molecular analysis of expression of pro and anti-apoptotic genes. Figure represent the level of mRNA expression of antiapoptotic genes (Bcl-2) and apoptotic genes (p53, Bax, Cas-3, Cas-8, NFkB and fas) were analyzed by semi-quantitative RT-PCR Where C, T and M indicates in untreated EAC Cells (control), nickel(ll) complex-treated EAC cells and molecular marker respectively. The position of the bands along with their length is indicated in bp. (a) Fragmentations of genomic DNA in EAC cells treated with 2.75 mg/kg b.wt of nickel(ll) complex for 5 consecutive days. (b) Isolated RNA from both control and treated EAC cells in 1% agarose gel electrophoresis. (c) GAPDH (housekeeping gene) expression as a control to normalize the expression levels of other genes where similar level of expression was observed in case of control and treatment. Up-regulation of the Proapoptotic gene Bax was found in compare to control as well as in p53. (d) Down regulation of the anti apoptotic gene BCl-2 in case of treated cells compare to control. (e) Initiator caspase-8 expressed more in comparison with control; in contrast NFkB expression was reduced. (f) Expression of the effector caspase, caspase-3 indicating the initiation of the apoptosis. (g) The expression of the Fas ligand was higher in case of nickel(ll) complex treated EAC cells which indicates the induction of the extrinsic pathway of apoptosis

synthesized nickel(ll) complex. This apoptotic pathway of complex is strongly supported by the previous study.[46]

3.12 | Determination of median survival time and percentage increase in life span

Mean survival time and life span of tumor-bearing mice were significantly expanded after nickel(ll) complex treatment (Figure 6). In fact tumor-bearing mice treated with complex at doses of 0.3 and 2.75 mg/kg resulted in significant increase of life span, namely 35.13 and 40.54%, respectively, compared with that of control mice ($p < 0.05$). On the other hand, mice treated with bleomycin increased life span by 94.59% in comparison with the control group (treated with solvent only).

3.13 | Hematological parameters

The hematological parameters were studied. Due to toxic effects of EAC cells in non-treated mice these parameters showed effect consistent with physiological deterioration as compared with the control group. However, these deteriorated parameters became upturned toward normal ranges when administration of nickel(ll) complex at the dose of 0.3 and 2.75 mg/kg b.wt/day was provided. Hematological parameters (Table 6) were studied in six groups of mice and each entry comprises six animals: normal

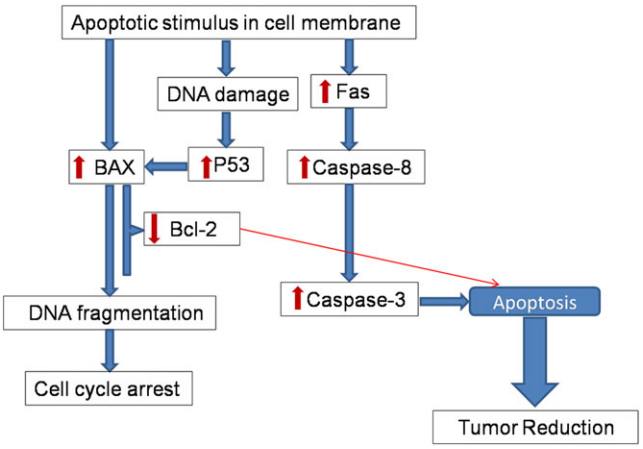

FIGURE 5 Apoptotic pathway of EAC cells treated with nickel(ll) complex. The complex can inhibit cells growth by initiating apoptosis via the above described pathway

mice (without any treatment), EAC-bearing control, EAC-bearing mice treated with bleomycin, ligand, and complex for 5 consecutive days. Blood was collected from the mice on 6th day of treatment and studied the blood parameters. All valued are shown as mean ± standard error of mean (SEM).

3.14 | Liver and kidney function test

The regular function of the two major organs such as liver and kidney was analyzed in both treated and non-treated mice by performing different blood biochemistry test. As determined for hematological parameters in non-treated EAC bearing mice, these parameters showed effect consistent with physiological deterioration as compared with the control mice. But these deteriorated parameter values came to near normal ranges when nickel(ll) complex was given to the animals at the dose of 0.3 and 2.75 mg/kg b.wt/day. Liver and kidney parameters (Table 7) were evaluated in six groups of mice (each of six animals). Beside normal mice (without any treatment) and EAC-bearing control, four groups were EAC-bearing mice treated with bleomycin, ligand, and complex for 5 consecutive days. At sixth day, the sample (blood) was collected and analyzed.

3.15 | *In vivo* toxicological assay

For evaluating drug-induced hepatotoxicity and nephrotoxicity, the levels of ALT, AST, ALP, bilirubin, urea

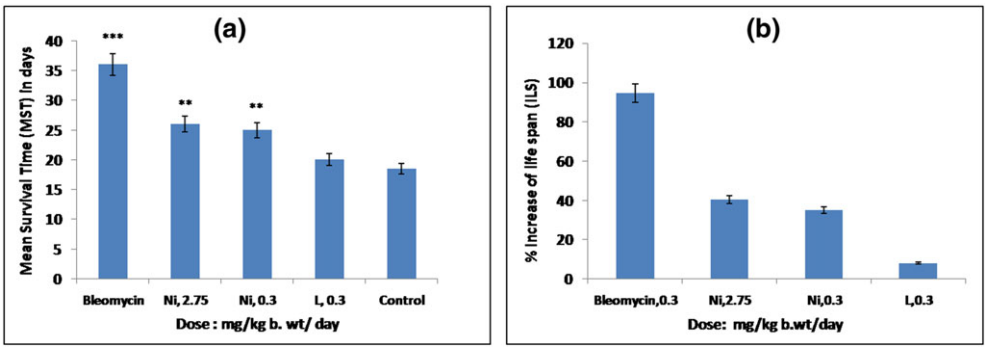

FIGURE 6 *In vivo* anticancer activities of Ligand (L) and nickel(ll) complex (Ni). (a) Mean survival time (b) Percentage of life span increase. Data expressed as mean ± SEM (n = 6). Level of significance *p < 0.05 and **p < 0.01 and ***p < 0.001 when compared with those of control group

TABLE 6 Effect of the ligand (L) and nickel(ll) complex (Ni) on hematological parameter in EAC bearing mice

Treatment and dose (mg/kg b. wt/day)	RBC (million cell/mm3)	WBC (million cell/mm3)	Hb (%) (gm/dL)
Normal control	51.16 ± 1.25	3568.66 ± 7.09	12.66 ± 2.08
EAC bearing control	27.09 ± 1.01	8248.33 ± 3.78	5.30 ± 0.57
EAC + Bleomycin (0.3)	49.33 ± 2.08	4229.00 ± 6.55	12.30 ± 0.58
EAC + L (0.3)	29.00 ± 2.00	5092.00 ± 6.42	6.00 ± 1.00
EAC + Ni (0.3)	37.66 ± 2.51	4514.33 ± 5.85	7.60 ± 0.57
EAC + Ni (2.75)	43.66 ± s1.52	4356.33 ± 4.04	10.33 ± 1.0

Each calculated values represent mean ± SEM (n = 6 mice per group); RBC, red blood cell; WBC, white blood cell; Hb, hemoglobin.

TABLE 7 Effect of the ligand (L) and nickel(ll) complex (Ni) on liver and kidney parameters in EAC bearing mice

	Liver function test				Kidney function test	
Treatment and dose (mg/kg/day)	**ALT (U/L)**	**AST (U/L)**	**ALP (U/L)**	**Bilirubin (mg/dL)**	**Urea (mg/dL)**	**Creatinine (mg/dL)**
Normal control (NC)	55	74	282	<0.10	34.24	0.4
EAC bearing control	185	433	140	0.15	36.38	0.4
EAC + L (0.3)	71	224	155	0.12	25.68	0.5
EAC + Ni (0.3)	68	198	185	<0.10	30.40	0.4
EAC + Ni (2.75)	63	172	192	<0.10	32.10	0.4

ALT, Alanine aminotransferase; AST, Aspartate aminotransferase; ALP, Alkaline phosphatase.

and creatinine obtained for the treated groups were compared with those of normal control (NC) mice (Table 7). It is worth noting that all the values come to near normal range in the metal complex treated groups. Histopathology of liver revealed that in both ligand and metal complex treated group's hepatocytes retained their normal architecture the sixth day. Mild inflammatory reactions at some portions of the hepatic parenchyma, pyknotic nucleus and vaculation were observed, (Figure 7c, d). However, any distention or obliteration wasn't observed in the central vein and hepatic sinusoids. Thus the test compound showed mild hepatotoxicity. Thus metal complex exhibited only mild hepatotoxicity in EAC bearing mice when used in the present dose schedule. Photomicrographs showed normal histological features in both kidneys from tumor control and treated mice (Figure 7). The cortex contained well-disposed renal corpuscles (i.e. intact Bowmans capsule and glomerulus), convoluted tubules and medullary rays. The inner medulla region contained the Henles loop and the collecting tubules. Therefore, the complex at the doses did not manifest nephrotoxicity. This observation was further supported by serum urea and creatinine assay.

4 | DISCUSSION

Cancers have a variety of strategies to escape cell death, together with changed expression of genes and proteins involved in cell survival.[47] Apoptosis is the best way of cell death by which the body selectively eliminates harmful or needless cells through a series of chronological actions without disturbing surrounding normal cells. Ceasing of apoptosis is the early incidence in tumor growth, which allows the cell to proliferate oddly and leading to the progression of cancer.[48] A general survival

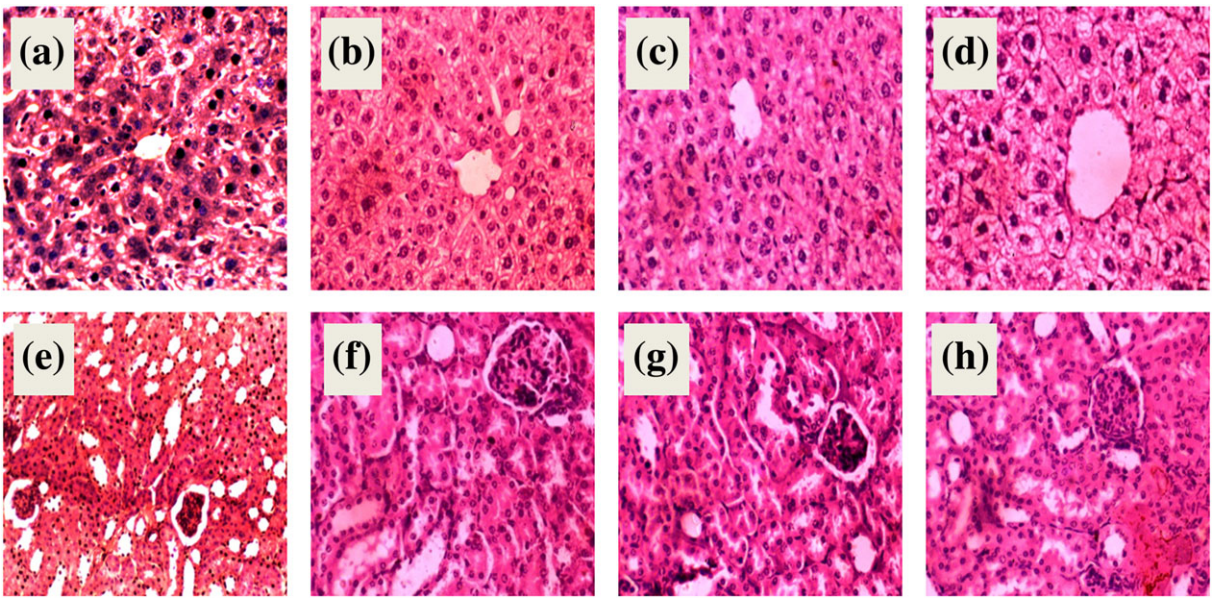

FIGURE 7 Photomicrographs of H/E-stained sections of liver and kidney of Swiss mice. (a) EAC control liver, (b) Normal liver (c) Ligand treated liver, (d) Metal complex treated liver. (e) EAC control kidney, (f) Normal kidney, (g) Ligand treated kidney, (h) Metal complex treated kidney (All pictures magnified × 40x)

strategy of reinstating or restoring normal cell apoptotic phenomenon may be by hyper-activation of pro-apoptotic genes[49] or deregulation anti-apoptotic genes Therefore, finding target selective therapeutic drugs is greatly related to the comprehensive conception of apoptotic signaling pathways.

Metal complex of dithiocarbazic acid and its Schiff base have been studied extensively because of their anticancer, antibacterial, antifungal, antiamoebic and insecticidal activities[50–52] Although the synthesis and complexation of S-benzyldithiocarbazate (SBDTC) and its derivatives have been under study for long since, considerable attention continues to be given to these and related ligands along with their metal complexes, since their atributes can be greatly modified by introducing different substituents.[52] For this reason, a new four coordinate labile nickel(ll) complex of tridentate ONS Schiff base ligand obtained from S-benzyl dithiocarbazate (SBDTC) with 2,4-dihydroxy benzaldehyde in the current project. As evident from X-ray crystallography result, the ligand coordinated nickel(ll) by thiolate sulfur, azomethine nitrogen, and phenolate oxygen atoms forming a four coordinate distorted square planar nickel(ll) complex, where the fourth site occupied by the nitrogen atom of acetonitrile used as solvent during crystallization. However, the mass spectrum in solution indicated that a DMSO molecule used as solvent replaced the acetonitrile ligand. This feature suggested the formation of a labile complex in solution thereby making it a potential biologically active compound able to interact with protein, DNA/RNA. Owing to its natural abundance in human and play vital role in cellular functions, nickel has been widely used in medicinal chemistry.[53,54]

In this work the cytotoxicity of the ligand and its nickel(ll) complex was estimated against Ehrlich Ascites Carcinoma cell (EAC) within concentration range 31.25–500 μg/ml. The IC_{50} values were calculated for the ligand and the complex and results are presented in Figure 2a and 2b. Cytotoxic activity of the metal complex may be imputed, as described by Tweedy's chelation theory.[55,56] According to this theory, chelation significantly reduces the polarity of the metal ion mostly because of partial sharing of its positive charge with the donor atoms and probable electron delocalization over the whole chelate ring. Such chelation could also develop the lipophilic nature of the central atom, which afterward favors its penetration through the lipid layer of the cell membrane. *In vivo* cytotoxicity results indicated that the tested complex revealed potent cytotoxic (% of cell growth inhibition 69.36) against EAC cells. It was marked that the metal complex is more effective than the free ligand, indicating an increase of the antitumor activity upon chelation. This result may be assigned to the positive charge of the metal that increases the acidity of the coordinated ligand bearing protons, and induces stronger hydrogen bonds.[57,58] A suitable choice of the nature of the metal ion anion and coordination geometry has a profound effect on the biological behavior of the complex by altering the binding ability to DNA.[59,60] Metal has been prompted oxidative tissue injury by the action of the free radical in definite pathway which is analogous to the Fenton reaction, as explained by Gaetke and Chow .[61] Earlier studies have confirmed the cytotoxic result of some nickel containing compounds such as nickel complex of thiosemicarbazones, nickel(ll) complexes with furanylmethyl and thienylmethyl dithiolenes [1,3-dithiole-2-one and 1,3-dithiole-2-thione], nickel chelates of 5-dimethylaminomethyl-2-thiouracil.[62,63]

In the present studies, it was confirmed that the treatment of nickel(ll) complex triggered morphological changes of EAC cells, including DNA fragmentation, cell shrinkage, and DNA condensation (Figure 3), which are the characteristic features of apoptosis.[64] These morphological changes were observed clearly while compared with untreated EAC cells.

It is well accepted that whether a cell becomes devoted to apoptosis partly depends upon the balance between proteins that mediate cell cycle arrest and cell death (e.g. p53 and Bax) and proteins that promote cell viability (e.g. Bcl-2).[65,66] Upon treatment for five consecutive days the synthesized complex, up regulates P^{53}, Bax, Cas-8, Cas-3 and Fas and down regulates NF-kB and Bcl-2 gene expression. P^{53} is the important factor of apoptosis next to DNA damage and cell cycle arrest[67] and binds to Bcl-2 family members, thus release Bax to convey an apoptotic signal to the mitochondria that finally leads to cell death.[68] Pro-apoptotic p53 signaling and anti-apoptotic NFκB signaling take vital roles in tumor growth and progression, and are involved in angiogenesis, metastasis, and cell survival.[69–71] In this work, results (figure 4) recommended that up regulation of p53 led to consequent binding and down regulation of Bcl-2 expression. Down regulation of Bcl-2 increases Bax, thus declining the Bcl-2/Bax ratio and promoting apoptosis and death. In view of that, a decrease in NFκB signaling was observed, which inhibits apoptosis by Bcl-2.[72] DNA fragmentation is the final yield of apoptosis and would be the outcome of catalytic behavior of executioner caspases (caspases-3). DNA fragmentation is another hall mark for apoptosis and our complex showed a successful behavior in this regard. Using above mentioned all the data, an apoptotic pathway was drawn by our newly synthesized nickel(ll) complex (Figure 5). The proposed pathway validates the existing model of Kim *et al.*.[46] Anticancer activities with negligible side effects of the synthetic complex were also proved in EAC-bearing mice by assessment of mean

survival time, the increasing rate of life span and hematological parameters. In each and every cases complex have shown significant result. Most of the anticancer drugs currently used are known to produce undesirable side effects such as hepatotoxicity and renal toxicity. The liver and kidney parameters of both treated and non-treated mice were studied. These parameters showed effect consistent with physiological deterioration as compared with the control mice. But these deteriorated parameter values came to near normal ranges when nickel(ll) complex supplementation was given to the animals. In histopathology study, there was no significant change in liver and kidney when compared with EAC control group. Therefore the nickel(ll) complex, thus raising the possibility to include in a therapeutic moiety.

5 | CONCLUSION

A novel nickel(ll) complex has been synthesized. The tridentate ONS ligand (H_3L) afforded a mononuclear distorted square planar labile complex with nickel(ll) in presence of acetonitrile as co-ligand. This metal complex precursor derived from S-benzyl dithiocarbazate may further be optimized as drug lead for successful utilization in the treatment of cancer.

ACKNOWLEDGEMENTS

University Grants Commission (UGC) supported this research work by providing a grant (Grant no: 917-5/52/UGC/Science 9/2015). The authors are thankful to Md. Ruhul Amin, Senior scientific officer, BCSIR laboratories, Bangladesh and Ifthekhar Md. Nur, Principal Instrument Engineer, Central Science Laboratory, Rajshahi University, Bangladesh for providing nanodrop, optical and fluorescence microscopy facilities to carry out the research work.

CONFLICT OF INTEREST

The authors have no conflict of interest.

AUTHORS CONTRIBUTIONS

MAR, MAAAAI and RZ developed the concept and designed experiments. RM, EZ and MCH carried out analytical assay. Statistical analysis was done by MSR. RZ and TN wrote the manuscript and MAR also checked and revised the manuscript.

ORCID

Md Abu Reza http://orcid.org/0000-0002-3146-2772

REFERENCES

[1] K. D. Mjos, C. Orvig, *Chem. Rev.* **2014**, *114*, 4540.

[2] V. Milacic, D. Chen, L. Ronconi, K. R. Landis-Piwowar, D. Fregona, Q. P. Dou, *Cancer Res.* **2006**, *66*, 10478.

[3] M. C. Lanier, M. Feher, N. J. Ashweek, C. J. Loweth, J. K. Rueter, D. H. Slee, J. P. Williams, Y. -F. Zhu, S. K. Sullivan, M. S. Brown, *Bioorg. Med. Chem.* **2007**, *15*, 5590.

[4] R. Poellot, T. Shuler, E. Uthus, F. Nielsen, Proceedings of the North Dakota Academy of Science (USA) **1990**.

[5] F. H. Nielsen, *J. Nutr.* **1980**, *110*, 965.

[6] D. E. Fenton, *Biocoordination chemistry*, Oxford University Press, Oxford **2001**.

[7] D. A. Vicic, W. D. Jones, *J. Am. Chem. Soc.* **1999**, *121*, 4070.

[8] A. Andrews, T. Lyons, T. O'Brien, *J. Chem. Soc. (Resumed)* **1962**, 1776.

[9] M. A. Halcrow, G. Christou, *Chem. Rev.* **1994**, *94*, 2421.

[10] S. Kirschner, Y. -K. Wei, D. Francis, J. G. Bergman, *J. Med. Chem.* **1966**, *9*, 369.

[11] C. Walsh, *Nature* **2001**, *409*, 226.

[12] Z. H. Chohan, M. Arif, M. A. Akhtar, C. T. Supuran, *Bioinorg. Chem. Appl.* **2006**, *2006*, 1.

[13] M. A. Ali, S. Livingstone, *Coord. Chem. Rev.* **1974**, *13*, 101.

[14] M. J. Campbell, *Coord. Chem. Rev.* **1975**, *15*, 279.

[15] S. Padhye, G. B. Kauffman, *Coord. Chem. Rev.* **1985**, *63*, 127.

[16] H. Stunzi, *Aust. J. Chem.* **1982**, *35*, 1145.

[17] C. Mügge, R. Liu, H. Görls, C. Gabbiani, E. Michelucci, N. Rüdiger, J. H. Clement, L. Messori, W. Weigand, *Dalton Transact.* **2014**, *43*, 3072.

[18] A. Garoufis, S. Hadjikakou, N. Hadjiliadis, *Coord. Chem. Rev.* **2009**, *253*, 1384.

[19] T. Ravoof, K. Crouse, E. Tiekink, M. Tahir, E. M. Yusof, R. Rosli, *Polyhedron* **2017**.

[20] A. Scozzafava, L. Menabuoni, F. Mincione, G. Mincione, C. T. Supuran, *Bioorg. Med. Chem. Lett.* **2001**, *11*, 575.

[21] B. Fischer, K. Kryeziu, S. Kallus, P. Heffeter, W. Berger, C. R. Kowol, B. K. Keppler, *RSC Adv.* **2016**, *6*, 55848.

[22] N. M. Salem, L. El-Sayed, M. F. Iskander, *Polyhedron* **2008**, *27*, 3215.

[23] E. Zangrando, M. Islam, M. A. -A. A. Islam, M. Sheikh, M. Tarafder, R. Miyatake, R. Zahan, M. Hossain, *Inorg. Chim. Acta* **2015**, *427*, 278.

[24] A. Altomare, G. Cascarano, C. Giacovazzo, A. Guagliardi, *J. Appl. Crystallogr.* **1993**, *26*, 343.

[25] C. Rigaku, Tokyo, **2009**.

[26] G. M. Sheldrick, *Acta Crystallogr., Sect. A: Found. Crystallogr.* **2008**, *64*, 112.

[27] D. Lorke, *Arch. Toxicol.* **1983**, *54*, 275.

[28] S. Henkelman, G. Rakhorst, J. Blanton, W. van Oeveren, *Mater. Sci. Eng., C* **2009**, *29*, 1650.

[29] S. R. Kabir, M. M. Nabi, A. Haque, R. U. Zaman, Z. H. Mahmud, M. A. Reza, *Phytomedicine* **2013**, *20*, 1288.

[30] S. Kabir, M. Abu Zubair, M. Nurujjaman, M. Azizul Haque, I. Hasan, M. Farhadul Islam, M. Tanvir Hossain, M. Anowar Hossain, M. Abdur Rakib, M. Alam, *Biosci. Rep.* **2011**, *31*, 465.

[31] F. Islam, J. A. Khanam, M. Khatun, N. Zuberi, L. Khatun, S. R. Kabir, M. A. Reza, M. Ali, M. Rabbi, V. Gopalan, *Phytother. Res.* **2015**, *29*, 573.

[32] F. Islam, H. Khatun, M. Khatun, S. M. M. Ali, J. A. Khanam, *Pharm. Biol.* **2014**, *52*, 281.

[33] A. Alam, H. Suzuki, T. Tsukahara, *Cell Biol. Intern.* **2010**, *34*, 631.

[34] J. Khanam, M. Islam, M. Jesmin, M. Ali, *J. Nat. Sci. Found. Sri Lanka* **2010**, *38*, 225.

[35] M. Ali, M. Jesmin, *J. Nat. Sci. Found. Sri Lanka* **2010**, *38*, 145.

[36] P. I. d. S. Maia, G. d. A. André, J. J. N. Silva, A. D. Andricopulo, S. S. Lemos, E. S. Lang, U. Abram, V. M. Deflon, *J. Inorg. Biochem.* **2010**, *104*, 1276.

[37] M. Begum, E. Zangrando, M. Howlader, M. Sheikh, R. Miyatake, M. Hossain, M. Alam, M. Hasnat, *Polyhedron* **2016**, *105*, 56.

[38] R. Takjoo, R. Centore, *J. Mol. Struct.* **2013**, *1031*, 180.

[39] M. A. Ali, T. S. Guan, P. Bhattacharjee, R. J. Butcher, Y. Li, *Transition Met. Chem.* **1996**, *21*, 351.

[40] M. A. Ali, A. H. Mirza, M. Nazimuddin, P. K. Dhar, R. J. Butcher, *Transition Met. Chem.* **2002**, *27*, 27.

[41] M. A. Ali, A. L. Tan, A. H. Mirza, J. H. Santos, A. H. B. H. Abdullah, *Transition Met. Chem.* **2012**, *37*, 651.

[42] M. T. H. Tarafder, M. A. Ali, N. Saravanan, W. Y. Weng, S. Kumar, N. Umar-Tsafe, K. A. Crouse, *Transition Met. Chem.* **2000**, *25*, 295.

[43] Z. Lu, C. White, A. L. Rheingold, R. H. Crabtree, *Inorg. Chem.* **1993**, *32*, 3991.

[44] M. Nazimuddin, M. A. Ali, F. E. Smith, M. A. Mridha, *Transition Met. Chem.* **1992**, *17*, 74.

[45] T. Mosmann, *J. Immunol. Methods* **1983**, *65*, 55.

[46] Y. Kim, R. Cerbo, C. Hah, K. Bahn, J. Kim, Y. Ha, *J. Food Sci.* **2008**, *73*.

[47] C. M. Croce, *N. Engl. J. Med.* **2008**, *358*, 502.

[48] J. M. Brown, L. D. Attardi, *Nat. Rev. Cancer* **2005**, *5*, 231.

[49] S. W. Fesik, *Nat. Rev. Cancer* **2005**, *5*, 876.

[50] M. R. Maurya, A. Kumar, A. R. Bhat, A. Azam, C. Bader, D. Rehder, *Inorg. Chem.* **2006**, *45*, 1260.

[51] K. Tampouris, S. Coco, A. Yannopoulos, S. Koinis, *Polyhedron* **2007**, *26*, 4269.

[52] M. Tarafder, T. -J. Khoo, K. A. Crouse, A. M. Ali, B. M. Yamin, H. -K. Fun, *Polyhedron* **2002**, *21*, 2691.

[53] J. Haribabu, K. Jeyalakshmi, Y. Arun, N. S. Bhuvanesh, P. T. Perumal, R. Karvembu, *RSC Adv.* **2015**, *5*, 46031.

[54] S. Liu, W. Cao, L. Yu, W. Zheng, L. Li, C. Fan, T. Chen, *Dalton Trans.* **2013**, *42*, 5932.

[55] A. Ramadan, *J. Inorg. Biochem.* **1997**, *65*, 183.

[56] B. Tweedy, *Phytopathology* **1964**, *55*, 910.

[57] G. Feng, J. C. Mareque-Rivas, N. H. Williams, *Chem. Commun.* **2006**, 1845.

[58] J. C. Mareque-Rivas, R. Prabaharan, S. Parsons, *Dalton Trans.* **2004**, 1648.

[59] G. Feng, J. C. Mareque-Rivas, R. Torres Martin de Rosales, N. H. Williams, *J. Am. Chem. Soc.* **2005**, *127*, 13470.

[60] N. A. Illán-Cabeza, A. R. García-García, M. N. Moreno-Carretero, J. M. Martínez-Martos, M. J. Ramírez-Expósito, *J. Inorg. Biochem.* **2005**, *99*, 1637.

[61] L. M. Gaetke, C. K. Chow, *Toxicology* **2003**, *189*, 147.

[62] Z. H. Chohan, A. U. Shaikh, C. T. Supuran, *J. Enzyme Inhib. Med. Chem.* **2006**, *21*, 733.

[63] Z. Afrasiabi, E. Sinn, W. Lin, Y. Ma, C. Campana, S. Padhye, *J. Inorg. Biochem.* **2005**, *99*, 1526.

[64] J. F. Kerr, A. H. Wyllie, A. R. Currie, *Br. J. Cancer* **1972**, *26*, 239.

[65] P. Giannakakou, R. Robey, T. Fojo, M. V. Blagosklonny, *Oncogene* **2001**, *20*, 3806.

[66] S. R. Chinni, Y. Li, S. Upadhyay, P. K. Koppolu, F. H. Sarkar, *Oncogene* **2001**, *20*, 2927.

[67] K. Nakano, K. H. Vousden, *Mol. Cell* **2001**, *7*, 683.

[68] J. Yu, L. Zhang, *Oncogene* **2009**, *27*, S71.

[69] M. Karin, Y. Cao, F. R. Greten, Z. -W. Li, *Nat. Rev. Cancer* **2002**, *2*, 301.

[70] W. Jochum, E. Passegué, E. F. Wagner, *Oncogene* **2001**, *20*, 2401.

[71] A. Garg, B. Aggarwal, *Leukemia* **2002**, *16*, 1053.

[72] C. Borner, *Mol. Immunol.* **2003**, *39*, 615.

SUPPORTING INFORMATION

Additional supporting information may be found online in the Supporting Information section at the end of the article.

How to cite this article: Zahan R, Rahi MS, Sheikh MC, et al. Design, synthesis and X-ray structural studies of novel [acetonitrile-benzyl-3-N-(2, 4 dihydroxyphenylmethylene) hydrazinecarbodithioato-κ3-N′, S, O] nickel(ll) complex that potently inhibit cell proliferation through regulation of apoptosis related genes. *Appl Organometal Chem*. 2018;e4601. https://doi.org/10.1002/aoc.4601